THE JOURNAL OF BIOLOGICAL CHEMISTRY
Vol. 280, No. 7, Issue of February 18, pp. 6005–6015, 2005
Printed in U.S.A.

Interaction of DNA Fragmentation Factor (DFF) with DNA Reveals an Unprecedented Mechanism for Nuclease Inhibition and Suggests That DFF Can Be Activated in a DNA-bound State*

Received for publication, November 18, 2004
Published, JBC Papers in Press, November 30, 2004, DOI 10.1074/jbc.M413035200

Christian Korn‡§, Sebastian R. Scholz‡§¶, Oleg Gimadutdinow‖, Rudi Lurz‡‡, Alfred Pingoud‡, and Gregor Meiss‡§§**

From the ‡Institute of Biochemistry, Justus-Liebig-University Giessen, 35392 Giessen, Germany, the ‖Institute of Genetics, Kazan State University, Remlevskaja 18-28, Kazan, Russia, and the ‡‡Max-Planck Institute for Molecular Genetics, Ihnestrasse 73, D-14195 Berlin-Dahlem, Germany

DNA fragmentation factor (DFF) is a complex of the DNase DFF40 (CAD) and its chaperone/inhibitor DFF45 (ICAD-L) that can be activated during apoptosis to induce DNA fragmentation. Here, we demonstrate that DFF directly binds to DNA *in vitro* without promoting DNA cleavage. DNA binding by DFF is mediated by the nuclease subunit, which can also form stable DNA complexes after release from DFF. Recombinant and reconstituted DFF is catalytically inactive yet proficient in DNA binding, demonstrating that the nuclease subunit in DFF is inhibited in DNA cleavage but not in DNA binding, revealing an unprecedented mode of nuclease inhibition. Activation of DFF in the presence of naked DNA or isolated nuclei stimulates DNA degradation by released DFF40 (CAD). In transfected HeLa cells transiently expressed DFF associates with chromatin, suggesting that DFF could be activated during apoptosis in a DNA-bound state.

DNA fragmentation is a biochemical hallmark of apoptotic cell death that can be achieved by the action of several nucleases involved in various apoptotic signal transduction pathways (1–4). Of paramount importance for cell autonomous apoptotic DNA degradation is the DNA fragmentation factor (DFF)[1] (5). DFF is a heterodimeric complex of the nuclease DFF40 (CAD) and its specific chaperone/inhibitor DFF45 (ICAD-L) (6, 7). During DFF40 (CAD) biosynthesis, DFF45 (ICAD-L) serves as a specific chaperone for the formation of a catalytically competent nuclease (8, 9). Once the complex between the nuclease and its chaperone/inhibitor is formed, the inhibitory subunit can be cleaved by caspase-3 or granzyme B and in turn dissociates from the nuclease (5, 10–12). The released nuclease is now able to participate in high molecular weight and nucleosomal apoptotic DNA fragmentation (13).

Although initially purified from cytosolic fractions of human and murine cell lines, several lines of evidence indicate that DFF can be a nuclear factor as well (1, 2, 6, 7, 14–16). DFF40 (CAD) and DFF45 (ICAD-L), but not the small isoform of the inhibitor DFF35 (ICAD-S), display nuclear localization signals (NLS) at their C termini that contribute in an additive manner to the nuclear accumulation of this nuclease/inhibitor complex (14, 17). Several nuclear proteins interact with and possibly regulate the activity of DFF40 (CAD), one such factor being topoisomerase IIα, implying a putative cooperation with DFF40 (CAD) in large scale chromosomal DNA fragmentation (18, 19). DFF40 (CAD) activity is also enhanced by architectural chromatin proteins such as histone H1 and HMGB1 and 2. For example, DFF40 (CAD) directly binds to histone H1, suggesting that this protein perhaps targets the nuclease to the DNA linker region where nucleosomal DNA fragmentation occurs (6, 19–21).

In the present study, we provide evidence that DFF in addition to the above mentioned interactions can directly interact with DNA *in vitro* without inducing DNA cleavage and is able to associate with chromatin in transfected HeLa cells. This is the first known case of a DNase-inhibitor complex in which DNA binding occurs but DNA cleavage is blocked. Intriguingly, DNA binding by DFF prior to or concomitant with its activation by caspase-3 stimulates the activity of the released nuclease DFF40 (CAD) on naked DNA and isolated nuclei, suggesting that during apoptosis nuclear DFF can be activated in a DNA-bound state.

MATERIALS AND METHODS

Bacterial and Mammalian Expression Vectors—Vectors for the expression of differentially tagged subunits of DFF in mammalian cells, pCI-EGFP-DFF40, pCI-GST-DFF45, and pCS2-MT-DFF40, were described previously (22). pcDNA-3.1-EGFP-DFF45 was constructed by inserting the cDNA of DFF45 into a modified pcDNA-3.1 vector, allowing expression of GFP fusion proteins. pEGFP-C2-CTCF was a kind gift from Ru Zhang (Institute for Genetics, JLU-Giessen).

For bacterial expression of DFF subunits, the following vectors were used: pGEX-2T-CAD and pACET-DFF45, allowing coexpression of GST-CAD and DFF45 in *Escherichia coli* as described elsewhere (22, 23). pET-Duet1-HisCAD, for the expression of N-terminally His-tagged CAD, was constructed by inserting CAD cDNA into the expression vector pET-Duet-1 (Merck Biosciences). pRSETB-ICAD-L (a kind gift from W. C. Earnshaw) was used to express His-tagged ICAD-L (24). His-tagged ICAD-S was expressed using vector pLK-His-ICAD-S as described previously (22).

* This work was supported by Grant Pi 122/16-3 from the Deutsche Forschungsgemeinschaft. The costs of publication of this article were defrayed in part by the payment of page charges. This article must therefore be hereby marked "*advertisement*" in accordance with 18 U.S.C. Section 1734 solely to indicate this fact.

§ Both authors contributed equally to this work.
¶ Member of the Graduiertenkolleg Biochemie von Nukleoproteinkomplexen.

** Supported by the Deutscher Akademischer Austausch Dienst.

§§ To whom correspondence should be addressed: Institute of Biochemistry, Justus-Liebig-University Giessen, Heinrich-Buff-Ring 58, D-35392 Giessen, Germany. Tel.: 49-641-99-35404; Fax: 49-641-99-35409; E-mail: gf45@uni-giessen.de.

[1] The abbreviations used are: DFF, DNA fragmentation factor; CAD, caspase-activated DNase; ICAD-L, inhibitor of CAD large form; ICAD-S, inhibitor of CAD small form; PIPES, 1,4-piperazinediethanesulfonic acid; CHAPS, 3-[(3-cholamidopropyl)dimethylammonio]-1-propanesulfonic acid; PBS, phosphate-buffered saline; NTA, nitrilotriacetic acid; EMSA, electrophoretic mobility shift assay; GST, glutathione *S*-transferase; Z, benzyloxycarbonyl; fmk, fluoromethylketone; GFP, green fluorescent protein.

Non-detergent Cell Lysis and Immunodetection of Endogenous DFF—Non-detergent cell lysis was performed using the CNM compartmental protein extraction kit (BioChain Institute, Inc.) according to the supplier's recommendations. Western blotting was performed using polyclonal anti-DFF40 and anti-DFF45/35 antibodies (ProSci, Inc.) in combination with horseradish peroxidase-conjugated secondary antibodies (Merck Biosciences-Calbiochem) and enhanced chemiluminescence detection reagents (ECL) (Amersham Biosciences).

Cell Culture and Transfection—Mammalian cells were cultured in a humidified atmosphere of 5% CO_2 in Dulbecco's modified Eagle's medium with 10% fetal calf serum, 100 units of penicillin, and 100 μg/ml streptomycin.

For *in situ* nuclear matrix preparations, HeLa cells were grown as described above on glass slides in 9.4-cm dishes and transfected by Ca^{2+}-phosphate co-precipitation using a total of 30 μg of DNA. For preparative nuclear matrix preparations, HeLa cells grown in maxidishes were transfected by calcium phosphate co-precipitation with 60 μg of DNA.

Nuclear Matrix Preparations—In situ nuclear matrix preparations were performed as described previously with a slight modification (25). HeLa cells transfected with appropriate GFP fusion constructs were extracted with 0.25% Triton X-100, instead of 1%, in CSK100 buffer (10 mM PIPES, pH 6.8, 0.3 M sucrose, 100 mM NaCl, 3 mM $MgCl_2$, 1 mM EGTA, 1.2 mM phenylmethylsulfonyl fluoride, protease inhibitor mixture) to account for the Triton X-100 sensitivity of DFF. Cells were examined with a Leica TCS4D confocal laser-scanning microscope as described previously (22).

For in-batch nuclear matrix preparations, transfected HeLa cells were incubated in 0.5% Triton X-100 in CSK100 buffer for 5 min on ice and then passed five times through a 22-gauge injection needle. Cellular debris was removed by centrifugation at 6000 rpm for 5 min, and the pellet washed with 1× CSK100 buffer. Matrix stabilization, chromosomal DNA cleavage, and chromatin depletion were achieved as described above. Chromatin-depleted nuclei were pelleted by centrifugation at 10,000 × *g* for 20 min and washed twice with CSK50 buffer. The Triton X-100 soluble fraction, matrix-stabilized nuclei, and chromatin-depleted nuclei were analyzed by immunoblotting using rabbit GFP antiserum (α-GFP; Invitrogen) and an anti-rabbit horseradish peroxidase-conjugated secondary antibody (Merck Biosciences-Calbiochem) in combination with enhanced chemiluminescence detection reagents (ECL) (Amersham Biosciences).

Production of Recombinant Proteins and in Vitro Mutagenesis—Recombinant His-tagged DFF was produced as described previously with minor modifications (23). Briefly, His-tagged DFF was expressed in *E. coli* BL21Gold (DE3) cells transformed with the two compatible plasmids pACET-DFF45 and pET-Duet1-HisCAD. The soluble protein fraction containing His-tagged DFF was purified by standard Ni^{2+}-NTA affinity chromatography. Eluted DFF was concentrated using centricon microconcentrators and subjected to anion-exchange chromatography using a Mono-Q HR 5/5 column. Bound protein was eluted in buffer A (20 mM HEPES-KOH, pH 7.4, 100 mM NaCl, 1 mM EDTA, 10% glycerol, 0.01% CHAPS, 10 mM dithiothreitol) using a 15-ml gradient of NaCl (100–300 mM) at a flow rate of 1 ml/min. Peak fractions of recombinant DFF were collected and concentrated as before in buffer A.

GST-tagged DFF containing wild-type CAD or the K155Q and H263N CAD mutants were produced as described before (23, 26). Where desired, GST-tagged DFF bound to glutathione-Sepharose 4-B beads in PBS was incubated with thrombin (50 units) overnight to remove the GST tag. The processed complex from the supernatant was purified by anion exchange chromatography as described above. Caspase-3 was expressed and purified as described before (23).

His-tagged ICAD-L was expressed using plasmid pRSET-ICAD-L (see above) and His-tagged ICAD-S as described elsewhere (22). Briefly, the proteins were first purified by standard Ni^{2+}-NTA affinity chromatography and further purified by anion-exchange chromatography similarly as described above.

Electrophoretic Mobility Shift Assays (EMSA)—Standard DNA binding reactions were performed for 30 min in shift buffer (20 mM HEPES-KOH, pH 7.4, 100 mM NaCl, 2 mM EDTA, 10% glycerol, 0.01% CHAPS) containing 12.5 ng/μl plasmid DNA (pBS-VDEX) and indicated amounts of proteins (see figures) in a final volume of 20 μl. Aliquots of the binding reactions were transferred into shift loading buffer (75% sucrose, 0.1% bromphenol blue), loaded onto 0.8% agarose gels containing 0.05 μg/ml ethidium bromide and separated by electrophoresis in TBE buffer (Tris borate/EDTA, pH 8.3). Aliquots of the binding reactions with PCR products were analyzed by electrophoresis on 6 or 5% polyacrylamide gels in TPE buffer (Tris phosphate, pH 8.2). The gels were stained with ethidium bromide.

UV Cross-linking—A-39 bp double-stranded oligodeoxynucleotide at a concentration of 5 μM with photoactivatable 5-iododeoxyuridine incorporated at three adjacent sites in the center of one DNA strand radioactively labeled with ^{32}P at its 5′-end was incubated with 5 μM DFF in buffer A. UV irradiation of the DFF-DNA complex with a helium/cadmium laser at 325 nm for 30 min was applied to induce cross-linking. Aliquots of the reaction mix were separated by PAGE and analyzed by autoradiography.

Transmission Electron Microscopy—Plasmid DNA and protein were incubated at 37 °C for 30 min in a 10-μl reaction volume containing 30 ng of DNA and different concentrations of DFF ranging from 0 to 300 ng (molar ratios of enzyme to DNA between 30:1 and 300:1) in shift buffer. Complexes were fixed with 0.2% (v/v) glutaraldehyde for 10 min at 37 °C and, after 3-fold dilution in 10 mM triethanolamine chloride, pH 7.5, and 10 mM $MgCl_2$, adsorbed to freshly cleaved mica. Micrographs were taken using a Philips CM100 electron microscope at 100 kV and a Fastscan CCD camera (Tietz Video and Image Processing Systems GmbH, Gauting, Germany).

Reconstitution of DFF—For reconstitution of DFF we activated GST-tagged DFF (5 μM final concentration) in shift buffer (see above) or shift buffer supplemented with Mg^{2+} (5 mM final concentration) containing plasmid DNA (pBS-VDEX, 12.5 ng/μl) with caspase-3, then added pan-caspase inhibitor z-VAD-fmk (88 μM final concentration) and substituted the reaction mix with recombinant ICAD-L or ICAD-S, respectively, at 15 and 30 μM final concentration, corresponding to 3- and 6-fold molar excess of inhibitory subunits over free nuclease. Aliquots of the reaction were mixed with shift loading buffer and analyzed by agarose gel electrophoresis in TBE buffer (Tris borate/EDTA, pH 8.3).

Time Order of Addition Experiments—To examine the cleavage activity of DFF premixed with DNA prior to caspase-3 activation, we incubated His-DFF (20 nM) with plasmid DNA (pBS-VDEX, 25 ng/μl) for 5 min, added recombinant caspase-3 and then stopped caspase-3 processing of DFF after 15 min by addition of the pan-caspase inhibitor z-VAD-fmk (Sigma-Aldrich). DNA cleavage was initiated by the addition of $MgCl_2$ to a final concentration of 5 mM. To analyze the cleavage activity of DFF activated by caspase-3 in the absence of DNA, we incubated recombinant DFF (20 nM) with caspase-3 for 15 min and stopped caspase-3 activation of DFF by adding pan-caspase inhibitor. Activated DFF was then incubated with DNA (pBS-VDEX, 25 ng/μl) for 20 min, and the cleavage reaction started by addition of $MgCl_2$ as above. To analyze DNA cleavage activity of DFF incubated with DNA concomitant with caspase-3 activation, we mixed DFF (20 nM), DNA (pBS-VDEX, 25 ng/μl), and caspase-3, stopped caspase-3 activation of DFF after 15 min by addition of pan-caspase inhibitor and then started the DNA cleavage reaction after a further 5 min incubation by addition of $MgCl_2$. Aliquots of the DNA cleavage reactions were taken at 0 (immediately after addition of $MgCl_2$), 1, 3, 9, and 15 min time points, loaded onto 0.8% agarose gels and analyzed by electrophoresis as described above. To quantify DNA cleavage, the decrease of the supercoiled plasmid DNA band in the gels was measured and transformed into relative cleavage rates. To use chromatin as substrate, nuclei were isolated from HeLa cells by standard centrifugation procedures using Tris-buffered saline (TBS, 50 mM Tris-HCl, 200 mM NaCl, 3 mM KCl, 0.02% sodium azide, pH 7.5) and a cell lysis buffer (0.325 M sucrose, 10 mM Tris-HCl, pH 7.8, 5 mM $MgCl_2$, 1% Triton X-100) and cleaved using 50 nM DFF.

RESULTS

Inhibited and Released DFF40 (CAD) but Not DFF45 (ICAD-L) Interact with DNA—In an attempt to identify the DNA binding domain of DFF40 (CAD) we to our surprise found that not only the released nuclease subunit itself but also the nuclease/inhibitor complex DFF forms stable DNA complexes *in vitro*. In the EMSA shown in Fig. 1*B*, we used GST-tagged wild-type DFF and the active site variant H263N of murine DFF40 (CAD) as well as recombinant DFF45 and GST with plasmid DNA as substrate. His^{263} is an important catalytic residue of murine DFF40 (CAD) situated in the active center close to the C terminus of the protein (Fig. 1*A*) (23, 27, 28). The H263N variant of murine DFF40 (CAD) was used to see, whether this catalytically inactive enzyme retains the ability to bind DNA despite of its inability to cleave it. Recombinant DFF45 and GST were analyzed for control. As shown in Fig. 1*B*, DFF and the nuclease subunits released from DFF, but neither the inhibitory subunit DFF45 nor GST, form stable DNA complexes. Formation of these complexes is not depend-

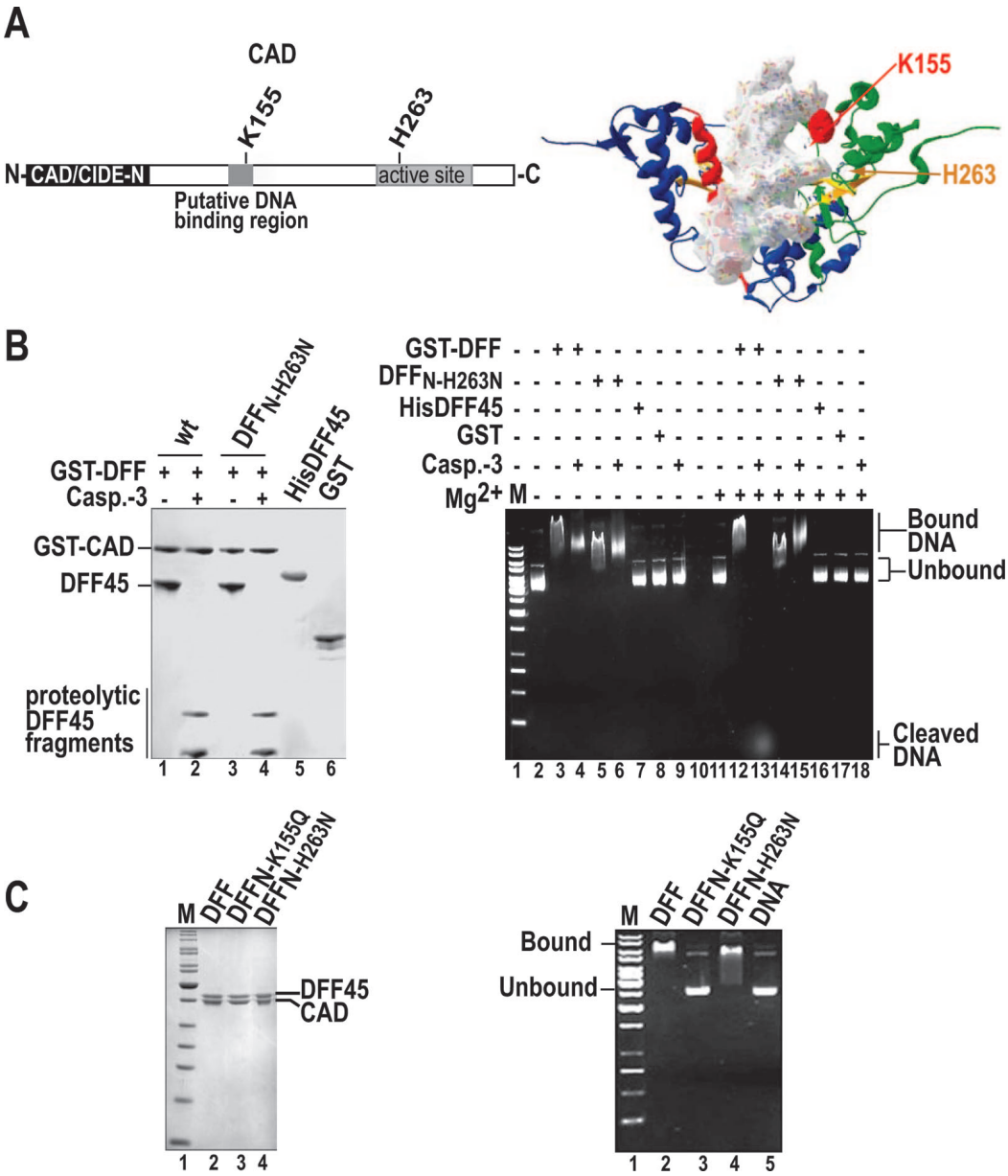

FIG. 1. *A*, scheme of CAD (murine DFF40) showing the positions of two critical amino acid residues (*K155* and *H263*) (*left panel*) and model for the CAD-DNA complex based on the crystal structure of active CAD (1v0d). His^{263} is located in the catalytic center (*highlighted in orange*) while Lys^{155} is buried at the N terminus of α-helix 4 (*highlighted in red*) that fits into the major groove of the DNA (CAD-DNA model has been adapted from Woo *et al.*, 28). The two identical subunits of the CAD dimer are highlighted in *blue* and *green*, respectively (*right panel*). *B*, SDS-PAGE of GST-tagged wild-type and mutant DFF as well as His-DFF45 and GST. Treatment of DFF with caspase-3 leads to proteolysis of the inhibitory subunit DFF45 (ICAD-L) and release of the nuclease DFF40 (CAD) (*left panel*). GST-DFF, $DFF_{N\text{-}H263N}$, and the nuclease released by caspase-3 treatment, but neither DFF45 nor GST, induce a mobility shift in the DNA (*right panel*). The inactive H263N-variant of CAD does not cleave the DNA in the presence of Mg^{2+} (*lane 15*) allowing sustained DNA complex formation under conditions where wild-type nuclease readily cleaves its substrate (*lane 13*). *Lanes*: *1*, marker; *2*, plasmid; *3*, GST-DFF; *4*, activated GST-DFF; *5*, GST-DFF H263N variant; *6*, activated GST-DFF H263N variant; *7*, His-DFF45; *8*, GST; *9*, caspase-3; *10*, empty lane; *11*, plasmid + Mg^{2+}; *12*, GST-DFF + Mg^{2+}; *13*, activated GST-DFF + Mg^{2+}; *14*, GST-DFF H263N variant + Mg^{2+}; *15*, activated GST-DFF H263N variant + Mg^{2+}; *16*, His-DFF45 + Mg^{2+}; *17*, GST + Mg^{2+}; *18*, caspase-3 + Mg^{2+}. *C*, SDS-PAGE of wild-type DFF and the variants $DFF_{N\text{-}K155Q}$ and $DFF_{N\text{-}H263N}$ with single amino acid substitution of Lys^{155} and His^{263} in DFF40 (CAD), respectively (*left panel*). EMSA shows that exchanging Lys^{155} with Gln in CAD abrogates the DNA binding abilities of DFF. In contrast to $DFF_{N\text{-}K155Q}$, $DFF_{N\text{-}H263N}$ still forms stable DNA complex similar to wild-type DFF (*right panel*).

ent on the presence of Mg^{2+}, which is an essential cofactor for DNA cleavage by the nuclease DFF40 (CAD) as seen in Fig. 1*B* (27). In the absence of Mg^{2+}, the wild-type nuclease and the H263N variant induce a similar mobility shift in the DNA. In the presence of Mg^{2+}, the wild-type nuclease readily cleaves the DNA, loosing its ability to induce a mobility shift (Fig. 1*B*, *lane 13*), whereas the active site variant H263N cannot cleave but can still bind the DNA (Fig. 1*B*, *lane 15*). These results clearly show that not only the nuclease subunit released from DFF but also the unprocessed nuclease/inhibitor complex DFF can form stable DNA complexes, which is highly unusual both for nonspecific nucleases and nuclease/inhibitor complexes. The data also suggest that the nuclease subunit in DFF mediates DNA binding of the nuclease/inhibitor complex, since the inhibitory subunit alone does not form DNA complexes (Fig. 1*B*, *lanes 7* and *16*). EMSA with a second inactive variant of murine DFF40 (CAD) with substitution of Lys^{155} by Gln supports this suggestion. Lys^{155} in murine DFF40 (CAD) is not an active site residue but closer to the CAD/CIDE-N-domain of the enzyme and appears to be involved in maintaining the protein

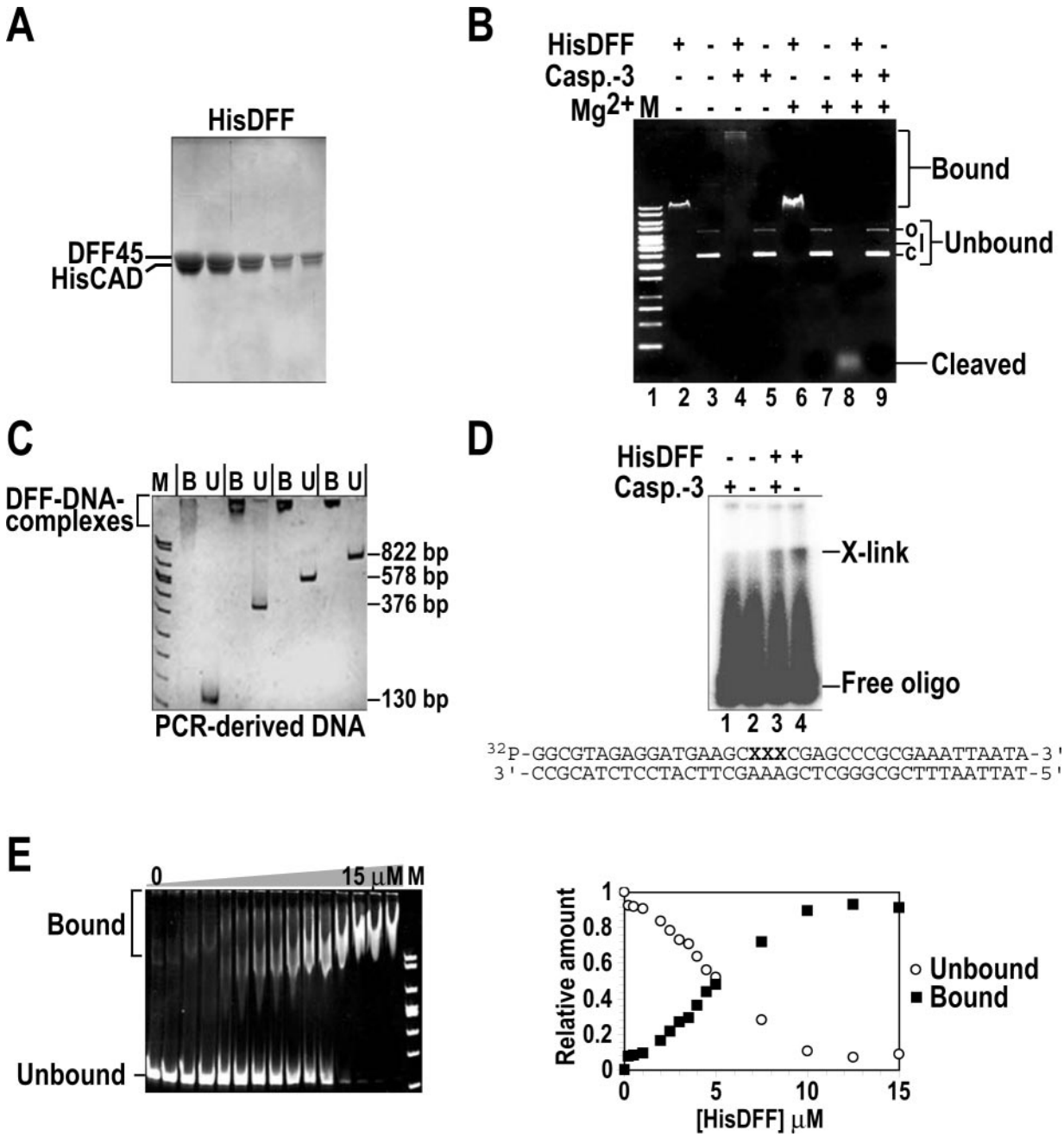

FIG. 2. *A*, recombinant His-tagged DFF was expressed and purified as described in "Materials and Methods." Based on SDS-PAGE and Coomassie staining, the protein complex is >95% pure. Shown are fractions containing HisDFF eluted from the Mono Q HR5/5 column. *B*, EMSA with plasmid DNA and His-tagged DFF. DFF (*lanes 2* and *6*) and the nuclease released (*lane 4*) induce a mobility shift in the DNA. In the presence of Mg^{2+} the nuclease cleaves the substrate without inducing a shift (*lane 8*). *C*, DFF binds PCR-derived DNA substrates of various lengths. EMSA with non-denaturing PAGE with PCR product sizes as indicated. Under the conditions applied, the DFF-DNA complex barely enters the gel matrix (6%) indicating a high molecular weight or aggregation (*B*, *bound; U*, *unbound; M*, *marker*). *D*, UV cross-linking experiment with DFF and caspase-3-activated DFF cross-linked to a radioactively labeled double-stranded 39-bp oligodeoxynucleotide with three central 5-iododesoxyuridine residues in one strand. Shown is the autoradiogram of the SDS-PAGE. *E*, titration of a 273-bp PCR-derived DNA substrate (12.5 ng/μl reaction mix) with recombinant His-DFF (0–15 μM final concentration). The reaction was analyzed by 5% PAGE (*left panel*). Quantitative evaluation reveals a dissociation constant for the DFF-DNA complex of approximately $K_d \approx 5 \times 10^{-6}$ M (*right panel*).

structure and/or DNA binding (Fig. 1*A*) (23, 26). In this EMSA we used thrombin-treated GST-DFF complexes in order to rule out that the binding activity seen is an artifact caused by the GST fusion (Fig. 1*C*). Interestingly, DFF with the K155Q mutant of CAD, $DFF_{N\text{-}K155Q}$, does not form stable DNA complexes whereas $DFF_{N\text{-}H263N}$ and wild-type DFF do (Fig. 1*C*). This corroborates that the nuclease subunit in DFF mediates DNA binding and suggests that Lys^{157} (Lys^{155}) in DFF40 (CAD) directly or indirectly plays an important role in DNA binding. The recently published crystal structure of murine DFF40 (CAD) illustrates that Lys^{155} is a buried residue stabilizing the N-terminal end of α-helix 4, which presumably binds in the major groove of the DNA (Fig. 1*A*) (28).

Recombinant DFF Binds to Various DNA Substrates in Vitro—So far our results revealed that DFF forms stable DNA complexes *in vitro* via its nuclease subunit DFF40 (CAD). In order to further characterize the DNA binding capacity of DFF we produced recombinant DFF with the nuclease subunit carrying an N-terminal extension of 12 amino acid residues [$MGRSH_6KL$] including a hexahistidine tag to facilitate puri-

fication and replacing the GST tag (Fig. 2*A*). This protein complex was used to carry out EMSA as well as UV cross-linking experiments with DFF and various DNA substrates including plasmid DNA as well as synthetic PCR products and oligodeoxynucleotides. As shown in Fig. 2*B*, His-tagged DFF, and the nuclease released from DFF by caspase-3 processing induce a mobility shift in the DNA. As seen from *lane 4* in Fig. 2*B*, nuclease released from DFF by caspase-3 treatment in the absence of Mg^{2+} led to high molecular weight complexes that stick to the wells of the agarose gel, which can be explained by the fact that released DFF40 (CAD) has the propensity to form oligomers (20, 29). Such high molecular weight DFF40 (CAD)-DNA complexes might be unable to enter the gel matrix. In some cases with free DFF40 (CAD) we also observed a smear instead of homogenous complex formation indicating a non-homogenous distribution of DNA complexes and suggesting that under the conditions applied the DFF40 (CAD)-DNA complexes are less stable than the DFF-DNA complexes. DFF also binds to synthetic DNA such as PCR products of various sizes (Fig. 2*C*) as well as to a 39-bp double-stranded oligodeoxynucleotide as demonstrated by UV cross-linking (Fig. 2*D*), apparently with a greater affinity toward larger DNA fragments. Titration of a 273-bp double-stranded PCR-derived DNA fragment with DFF in the presence (data not shown) or absence of Mg^{2+} revealed a dissociation constant $K_d \approx 5 \times 10^{-6}$ M (Fig. 2*E*). The sequences of the plasmid DNA, PCR products, and the oligodeoxynucleotide were unrelated, indicating that, as expected for a nonspecific nuclease, DFF binding to DNA is not sequence specific.

Visualization of DFF-DNA Complex Formation and DNA Cleavage by Transmission Electron Microscopy—In order to obtain additional information about the nature of the DFF-DNA complexes formed we analyzed DNA binding and cleavage by DFF using transmission electron microscopy. When plasmid DNA was incubated with increasing amounts of DFF at physiological salt concentration the decrease in electrophoretic mobility of the DFF-DNA complex compared with the free plasmid DNA analyzed by EMSA was dependent on the concentration of DFF (Fig. 3*A*). When such complexes were analyzed by transmission electron microscopy, similar results were obtained (Fig. 3*A*). Depending on concentration, DFF binds to plasmid DNA in a nonspecific manner, independent of the absence or presence of Mg^{2+}. As seen from Fig. 3*A*, DFF forms large aggregates on the DNA rather than sitting side by side on its substrate and more than one plasmid molecule is bound by such aggregates. When the nuclease subunit released from DFF by caspase-3 treatment was analyzed in the same way (Fig. 3*B*), we again observed nonspecific DNA binding in the absence of Mg^{2+} but, as expected, cleavage of the DNA into short linear fragments in the presence of Mg^{2+}, corroborating the results obtained from the gel shift experiments.

Recombinant and Reconstituted DFF Allow Formation of Stable DFF-DNA Complexes—Our results indicated that the free nuclease released from DFF and recombinant DFF obtained from co-expression of its subunits interact with DNA. It was pertinent to investigate if reconstitution of DFF, *i.e.* addition of inhibitory subunit to the nuclease subunit released from activated DFF results in the restoration of a DNA binding proficient but catalytically deficient nuclease/inhibitor complex. To this end, we have activated recombinant DFF using caspase-3, then added the pan-caspase inhibitor z-VAD-fmk and finally supplemented the reaction mixture with recombinant ICAD-S (DFF35) or ICAD-L (DFF45) again (Fig. 4*A*). As shown, reconstituted DFF is able to bind to the DNA substrate similar to recombinant DFF obtained from co-expression of its subunits, allowing formation of a stable DNA complex but

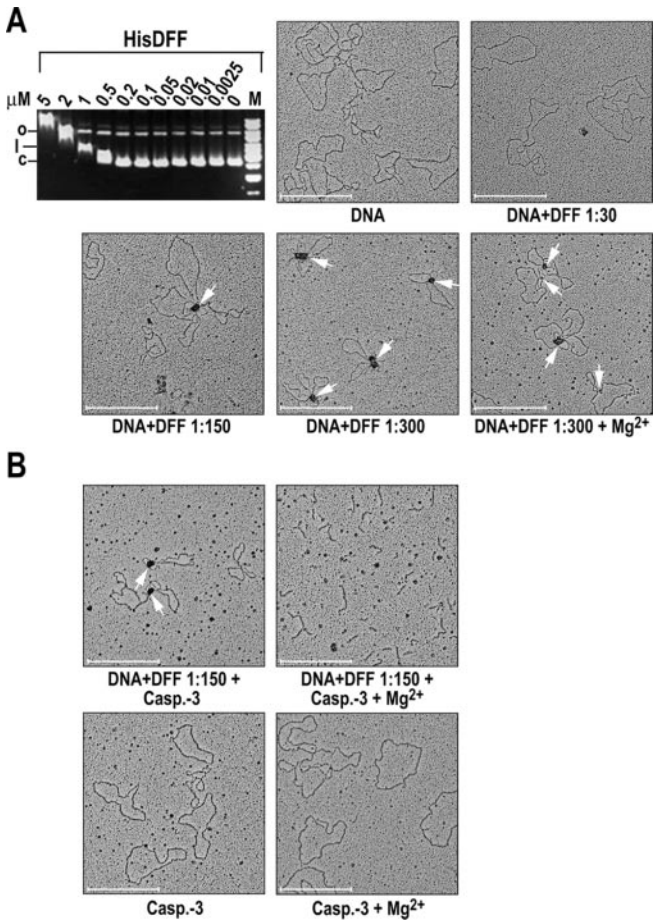

FIG. 3. *A*, DFF binds to plasmid DNA in a concentration dependent manner inducing a mobility shift when analyzed by EMSA (*left panel*) and forming large aggregates at high concentration on the DNA as seen on the microcraphs (*indicated by white arrows*). EMSA and transmission electron microscopy were performed under similar conditions. In the EMSA the molar excess of DFF over DNA is ~500-fold at 5 μM DFF. The numbers given under each micrograph indicate the molar ratio of DNA to DFF (ranging from 1:30 to 1:300) in the microscopic analysis. The *white bar* corresponds to 500 nm. *B*, DFF40 (CAD) released from DFF by caspase-3 treatment binds to DNA in the absence of Mg^{2+} (indicated by *white arrows* on the *top left panel*) but cleaves the DNA in the presence of Mg^{2+} (*top right panel*). Caspase-3 alone irrespective of the absence or presence of Mg^{2+} does not bind or cleave the DNA (*bottom panels*). The *white bar* corresponds to 500 nm.

inhibiting the activity of the nuclease subunit (Fig. 4*B*). When the reconstituted DFF complexes were activated by excess caspase-3 (indicated by *asterisks* in Fig. 4), DNA cleavage by DFF40 (CAD) was regained. This result clearly shows that inhibition of the nuclease subunit in DFF is due to blocking the catalytic activity but not the DNA binding capacity of DFF40 (CAD). The results also suggest that ICAD-S (DFF35) and ICAD-L (DFF45) use the same mechanism for inhibition of DFF40 (CAD). To our knowledge, this mode of nuclease inhibition has not been seen yet with any other known nuclease/inhibitor complex (see below).

DNA Binding by DFF Stimulates the Activity of Released DFF40 (CAD)—To elucidate if binding of DFF to DNA prior to or concomitant with its activation by caspase-3 has an influence on the activity of DFF40 (CAD), we performed time order of addition experiments. We compared the DNA cleavage kinetics of DFF40 (CAD) released from DFF incubated with DNA prior to or concomitant with its activation by caspase-3 with DNA cleavage kinetics of DFF40 (CAD) released from DFF activated by caspase-3 in the absence of DNA. Under the conditions applied, incubation of DFF with DNA prior to or con-

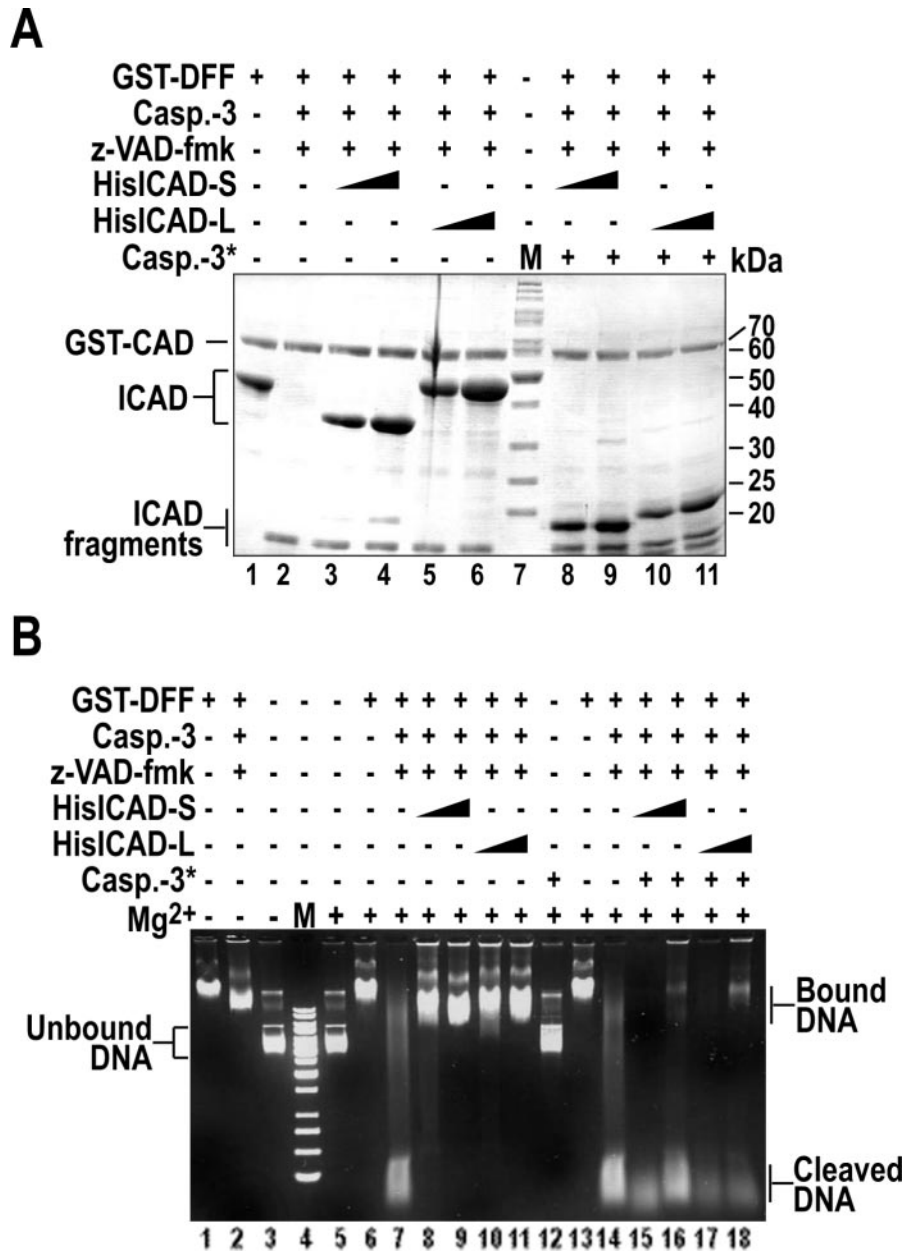

FIG. 4. *A*, SDS-PAGE of recombinant and reconstituted DFF used in the EMSA. *1*, GST-DFF; *2*, caspase-3 activated GST-DFF + pan-caspase-inhibitor; *3* and *4*, same as 2 + 3-fold and 6-fold molar excess of His-ICAD-S; *5* and *6*, same as 2 + 3-fold and 6-fold molar excess of His-ICAD-L; *7*, marker; *8–11*, same as 3–6 but reactivated with excess caspase-3. *B*, addition of ICAD-S (DFF35) or ICAD-L (DFF45) to the nuclease DFF40 (CAD) released from GST-DFF results in reconstitution of a DNA binding proficient but catalytically inactive DFF. Shown are the results of EMSA with plasmid DNA. *1*, GST-DFF; *2*, caspase-3 activated GST-DFF + pan-caspase-inhibitor; *3*, plasmid only; *4*, marker; *5*, plasmid + Mg^{2+}; *6*, GST-DFF + Mg^{2+}; *7*, caspase-3 activated GST-DFF + pan-caspase-inhibitor + Mg^{2+}; *8–11*, activated GST-DFF + pan-caspase inhibitor + HisICAD-S or HisICAD-L in 3-fold and 6-fold molar excess over DFF40 (CAD); *12*, plasmid + Mg^{2+} + caspase-3; *13*, GST-DFF + Mg^{2+}; *14*, caspase-3 activated GST-DFF + pan-caspase-inhibitor + Mg^{2+}; *15–18*, same as *8–11* but reactivated with excess caspase-3. The *asterisk* indicates addition of excess caspase-3.

comitant with its activation by caspase-3 clearly stimulated the activity of released DFF40 (CAD) (Fig. 5*A*). This suggests that activation of DNA-bound DFF leads to an apparently higher cleavage efficiency of the released nuclease subunit compared with the nuclease released in the absence of DNA. When the experiment was conducted with isolated HeLa cell nuclei as substrate we also observed a difference in the cleavage activity of DFF activated in the presence or in the absence of this substrate (Fig. 5*B*), indicating a similar behavior of DFF when bound to naked DNA or to chromatin substrates. To see whether the nuclease released from caspase-3-treated DFF is stable and retains its activity during the time order of addition experiments, we incubated activated DFF for defined time intervals at 37 °C and measured its residual nuclease activity in a hyperchromicity assay using high molecular weight salmon sperm DNA as substrate. As shown in Fig. 5*C*, incubation of the released nuclease up to 30 min at 37 °C does not lead to a detectable decrease in nuclease activity, ruling out that the drop in activity seen with DFF activated in the absence of DNA is caused by protein instability. In order to find out whether the different DNA cleavage rates observed upon activation of DFF were caused by a difference in the rate of activation of DNA-bound and -unbound DFF by caspase-3, we analyzed the proteolytic processing of DFF in the presence or absence of DNA by SDS-PAGE. As a result, the rate of DFF processing by caspase-3 is not influenced by the absence or presence of DNA, ruling out an enhancement of DNA cleavage activity due to a higher rate of proteolytic activation of DNA-bound DFF (Fig. 5*D*).

DFF Can Associate with Chromatin in Transfected HeLa Cells—Having shown that DFF interacts with DNA *in vitro* the question arises whether this nuclease/inhibitor complex can also associate with chromatin *in vivo*. To investigate a putative chromatin association of DFF, we first studied the localization of endogenous DFF in HeLa cells using a non-detergent lysis method for cell fractionation, since it has been shown previously that DFF readily leaks out of the nuclei upon treatment with detergents (15, 29). Western blotting of total lysate and cytosolic and nuclear fractions with antibodies against DFF40 and DFF45/35 revealed that in HeLa cells endogenous DFF is almost entirely located to the nucleus (Fig. 6*A*). Transfection of HeLa cells with constructs encoding green fluorescent protein (GFP) fusions of the human DFF subunits DFF45 or DFF40 in

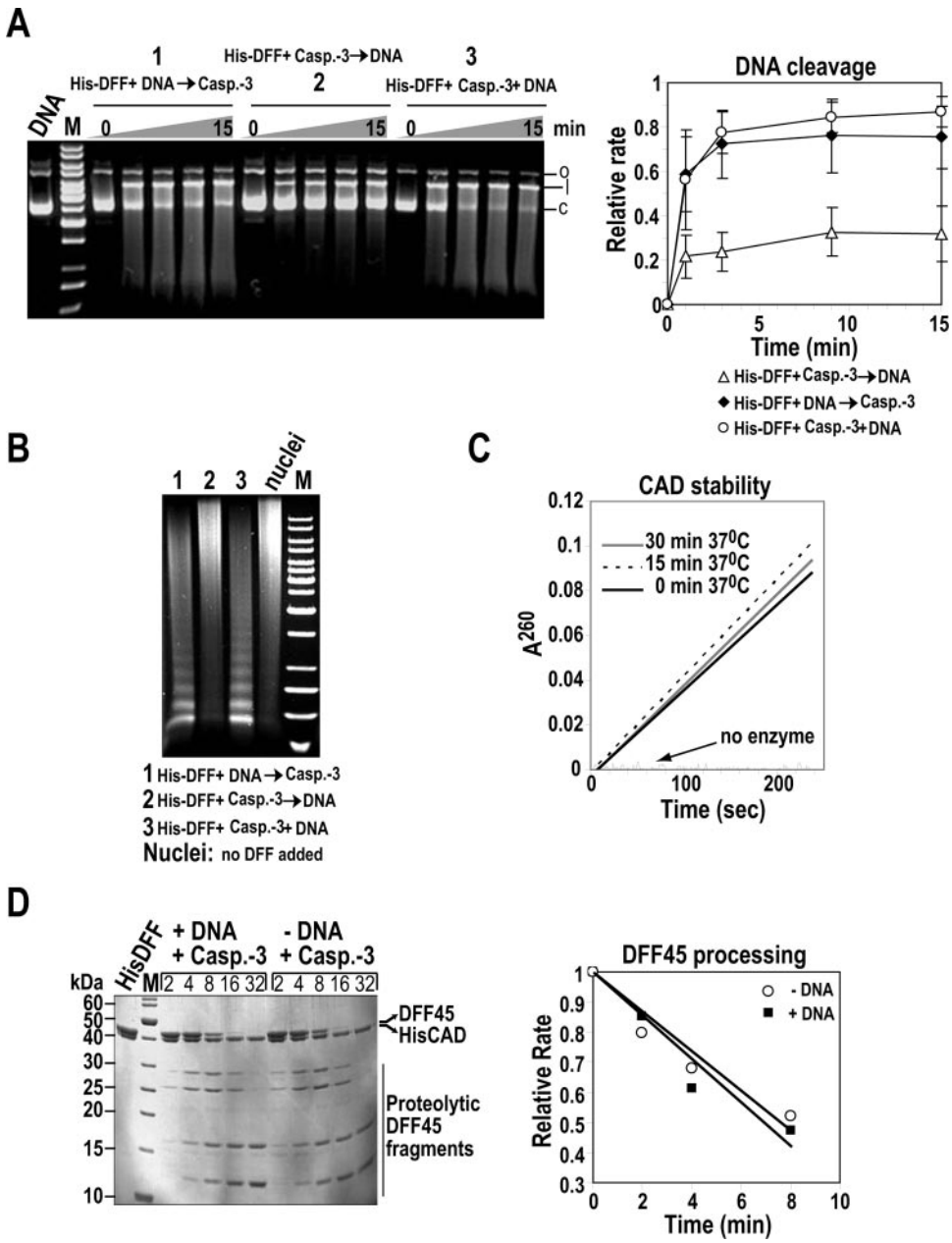

FIG. 5. *A*, comparison of plasmid DNA cleavage kinetics with DFF40 (CAD) released from DFF incubated with DNA prior or concomitant to activation by caspase-3 or activated in the absence of DNA. DFF40 (CAD) released from DFF in the presence of DNA has a higher activity (*1* and *3*) than nuclease released from DFF in the absence of DNA (*2*). Gel data of three independent time orders of addition experiments is plotted on *right*. *B*, same experiment as in *A* with nuclei isolated from HeLa cells as substrate. *C*, DFF40 (CAD) released from activated DFF and stored at 37 °C for 0, 15, and 30 min does not show a decrease in nucleolytic activity as determined in a hyperchromicity assay using salmon sperm DNA as substrate. *D*, comparison of the rate of proteolytic processing by caspase-3 of DFF in the presence or absence of DNA analyzed by SDS-PAGE (*left panel*) reveals no significant difference. Gel data plotted on *right panel*.

combination with their non-GFP-tagged counterparts confirmed the nuclear localization of transiently expressed DFF and its subunits (Fig. 6*B*). Nuclear localization was only abrogated when the NLS of either DFF45 (DFF45Δ323–331) or DFF40 (DFF40Δ329–338) was deleted (data not shown). Such complexes were then found predominantly in the cytoplasm, as shown previously (14). By extracting the DNA of transfected cells 72-h post-transfection, we were able to detect significant levels of DNA laddering in cells expressing tagged DFF but much less DNA laddering in cells transfected with DFF45 only (data not shown). When purified from transfected cells via GST pull-down, GST-DFF45/GFP-DFF40 complexes show DNase activity after caspase-3 activation *in vitro* (Fig. 6*C*), indicating that the tagged DFF complex is functional, both *in vivo* and *in vitro*.

After confirming that endogenous and transiently expressed DFF in HeLa cells can be found in nuclei, we investigated the subnuclear distribution of the complex by comparative *in situ* and preparative nuclear matrix assays essentially as described earlier (25). Because of the known detergent sensitivity of DFF, we modified the assay by reducing the Triton X-100 concentration from 1 to 0.25% and compared the relative Triton X-100 sensitivity of GFP-tagged DFF at this low concentration of detergent with that of GFP-DFF45, a presumed negative control, and GFP-CTCF (CCCTC-binding factor), a nuclear matrix-binding protein, serving as a positive control (30). For *in situ* nuclear matrix preparations transfected cells were either left untreated or were carefully treated with mild concentrations of Triton X-100, sodium tetrathionate, and/or DNase I to deter-

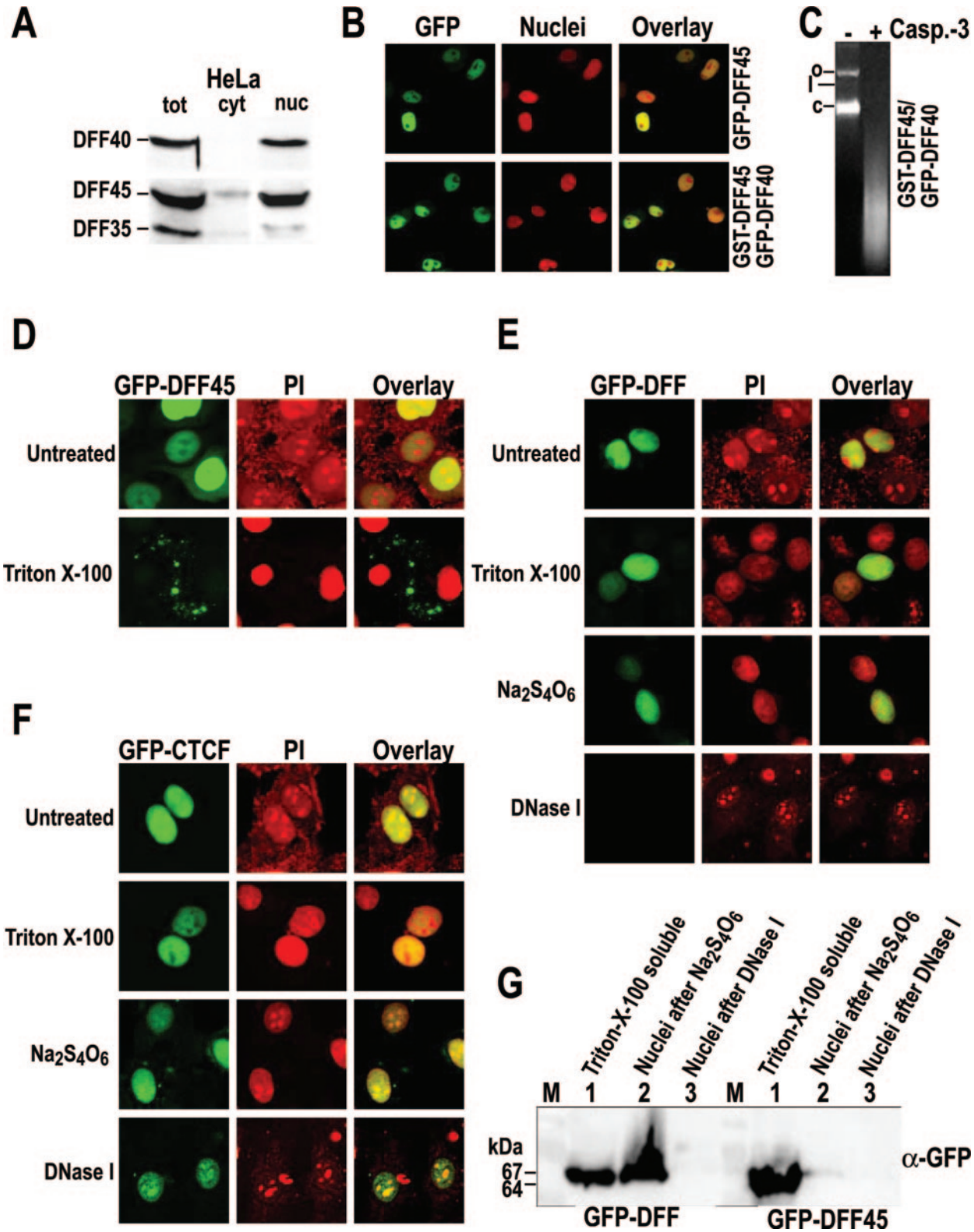

FIG. 6. *A*, Western blot using anti-DFF40 and anti-DFF45/35 antibodies after biochemical fractionation of HeLa cells by a non-detergent lysis method. Endogenous DFF subunits can be found in the nucleus (*tot*, total cellular extract; *cyt,* cytosolic fraction; *nuc*, nuclear fraction). *B*, GFP-tagged DFF45 (*upper panels*) and GFP-tagged DFF40 in complex with GST-tagged DFF45 (*lower panels*) are nuclear in transfected HeLa cells. Nuclear counterstaining was achieved by co-expression of a nuclear DsRed-Express variant. *C*, GFP-tagged DFF40 purified from transfected cells via GST-tagged DFF45 by GST-affinity chromatography is active *in vitro* after activation by caspase-3 as shown by cleavage of plasmid DNA (*o*, open circular; *l,* linear; *c,* supercoiled). *D*, inhibitor GFP-DFF45 expressed in transfected HeLa cells is readily washed out of the nucleus when cells are treated with the detergent Triton X-100 (*PI*, propidium iodide). *E*, heterodimeric nuclease/inhibitor complex DFF visualized by GFP fusion to the nuclease subunit can still be found in the nuclei after Triton X-100 and $Na_2S_4O_6$ treatment of the cells, but is absent from nuclei after chromatin depletion with DNase I. *F*, CTCF associates with the nuclear matrix. *G*, preparative nuclear matrix assay reveals that expressed DFF is found in the Triton X-100 soluble fraction and in the $Na_2S_4O_6$ stabilized nuclei in equal amounts. After chromatin depletion with DNase I, no DFF can be detected in the nuclei. In the case of DFF45, the protein is only found in the Triton X-100 soluble fraction.

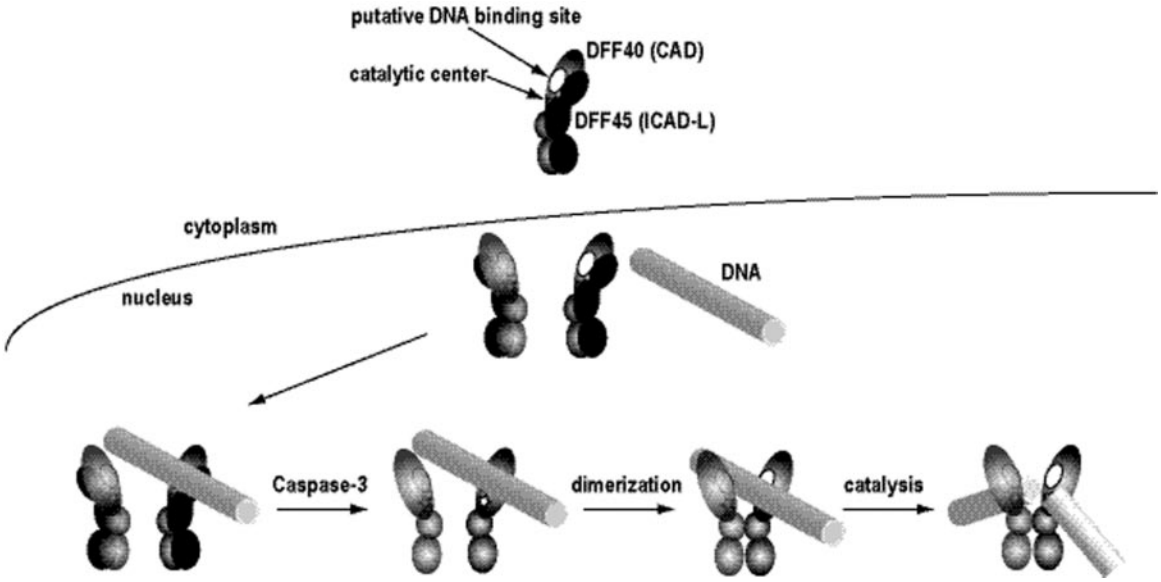

FIG. 7. **DFF can be found in the cytoplasm and nuclei of mammalian cells, dependent on the cell line.** According to our results, DFF directly binds to DNA via the nuclease subunit. Preformation of DFF-DNA complexes, *i.e.* the interaction of DFF40 (CAD) with DNA in the inhibited state, facilitates access of the DNA substrate to the catalytic center at the bottom of a deep active site cleft seen in dimeric CAD, probably by dimer assembly around the DNA.

mine whether the proteins are found in the Triton X-100-soluble fraction, associated with the chromatin or the nuclear matrix. When left untreated we found all the different fusion proteins, *i.e.* GFP-DFF45 (Fig. 6*D*), GFP-DFF (Fig. 6*E*), and GFP-CTCF (Fig. 6*F*) located in the nuclei. When transfected cells were subjected to treatment with mild concentrations of Triton X-100, DFF45 was readily washed out of the nuclei whereas the DFF complex and CTCF were still detectable there. When cells were also treated with sodium tetrathionate stabilizing the nuclear matrix, the presence of DFF and CTCF in the nuclei remained unaffected. However, when cells were subjected to detergent lysis, matrix stabilization, and DNase I treatment, DFF was absent from the chromatin-depleted nuclei (Fig. 6*E*) whereas CTCF, as expected, was found associated with the remaining nuclear matrix (Fig. 6*F*). A preparative nuclear matrix assay performed with DFF and DFF45 alone confirmed these results. More than 95% of DFF45 was detectable in the Triton X-100 soluble fraction, whereas DFF was split among the Triton X-100 soluble fraction and the chromatin fraction (Fig. 6*G*). Taken together, these results strongly suggest that the nuclease/inhibitor complex DFF, but not the inhibitory subunit DFF45 (ICAD-L) alone, is able to associate with chromatin corroborating the observations made on DNA binding by DFF *in vitro*.

DISCUSSION

DFF40 (CAD) is a nuclease that degrades chromatin during apoptosis by attacking phosphodiester bonds of DNA in the linker region between nucleosomes (5, 7). Cleavage restricted to the internucleosomal DNA in chromatin leads to the highly defined DNA laddering observed upon activation of DFF40 (CAD) during apoptosis. On naked DNA the enzyme acts as a nonspecific nuclease attacking almost every phosphodiester bond without sequence specificity but with some preference for AT-rich regions (19). Such sequence preferences have been found in many other nonspecific nucleases, *e.g.* DNase I (31) or endonuclease G (32, 33). Because of their inherent nonspecific character these nucleases usually do not show tight substrate binding and their interaction with DNA is mainly determined by contacts to the phosphodiester backbone, whereas interaction with the bases usually is rare (34–37). Our results now show that although acting as a nonspecific nuclease DFF40 (CAD) is able to form stable DNA complexes *in vitro*, independent of the presence or absence of a divalent metal ion cofactor, such as Mg^{2+}. This clearly differentiates DFF40 (CAD) from other nonspecific nucleases such as DNase I, endonuclease G or colicins E7/E9. As an exception, the latter DNase that acts as a bacterial toxin has been shown to form DNA complexes but only in the presence of Mg^{2+} and only when present as an inactive variant (38).

The most striking difference that highlights a unique feature of DFF40 (CAD) is the mechanism of inhibition of this particular nuclease by the inhibitory proteins DFF45/35 (ICAD-L/-S) compared with the inhibition of other nonspecific nucleases such as the RNases barnase and RNaseA or the bacterial DNase colicins E7/E9 (39–42). All these nucleases have to be tightly regulated in a cell to avoid accidental destruction of the genetic material ultimately causing cell death and one way of regulating these enzymes is complex formation with inhibitory factors (43). Although using different mechanisms of inhibition in detail, all the nuclease/inhibitor complexes mentioned above obey a common principle: they function by prohibiting the binding of nucleic acid substrates to the nuclease subunits thus preventing substrate cleavage. For example, in the colicins E9 and E7, which are inhibited by their corresponding immunity proteins Im9 and Im7, a so called exosite mechanism of inhibition is found in which the immunoprotein only partially occludes the active site of the DNase yet at the same time changes the electrostatic environment of this region leading to repulsion of a putative DNA substrate (36, 44–46). In the present study, our results indicate a very different mechanism for inhibition of DFF40 (CAD), in which cleavage of the DNA substrate is prevented but binding to the DNA occurs in the presence of the inhibitory subunit ICAD. In the absence of a crystal structure of the DFF complex it cannot be explained in detail how the inhibitory subunits DFF45/35 (ICAD-L/S) achieve to block catalysis of phosphodiester bond cleavage by DFF40 (CAD) but at the same time allow for substrate binding. For example, there could be an unblocked, non-catalytic DNA binding site in the nuclease subunit of the DFF complex in addition to a physically distinct catalytic center that is blocked

by the inhibitor. An equally likely scenario is that non-catalytic DNA binding and subsequent catalysis take place at a single site, the active site of the nuclease itself. This requires an active site cleft accommodating non-catalytic binding in the presence of inhibitor and binding and catalysis in the absence of inhibitor. In either case, the active site has to be blocked in such a way as to avoid catalysis. The fact that recombinant DFF and DFF reconstituted by complex formation of the released nuclease with DFF45 (ICAD-L) or DFF35 (ICAD-S) show a similar behavior in DNA binding further indicates that both isoforms of the inhibitor block DFF40 (CAD) activity in a similar way. Interestingly, our reconstitution experiments indicate that ICAD-S is a slightly more effective inhibitor of DFF40 (CAD) than DFF45 (ICAD-L), in agreement with previous observations (47, 48).

The very deep active site cleft formed by the two identical subunits of an active DFF40 (CAD) dimer as seen in the crystal would in theory allow a two stage binding mechanism, where in a first, non-catalytic stage, DNA is bound but not hydrolyzed and in a subsequent second stage, after activation, phosphodiester bond cleavage takes place (28). However, since in DFF the inhibitor is presumed to keep DFF40 (CAD) in a monomeric state, the active site cleft as described above is not formed (28). Since it is nevertheless seen from our experiments that DFF interacts with DNA it has to be assumed that a single DFF40 (CAD) molecule in the heterodimeric nuclease/inhibitor complex is sufficient to allow for non-catalytic DNA binding. The crystal structure of CAD shows that the active site residues of this enzyme are located in a $\beta\beta\alpha$-Me-finger-like motif that faces the DNA via the minor groove (28, 36, 37, 49). The CAD-DNA model also illustrates that the long α-helix 4 of DFF40 (CAD) very likely binds in the major groove of the DNA (28). It is therefore tempting to speculate that inhibited DFF40 (CAD) in DFF binds to the DNA via the major groove and provides a sufficiently stable interaction to form a DFF-DNA complex, while the catalytic center itself is blocked by the inhibitory subunit. Binding through the minor groove by the $\beta\beta\alpha$-Me-finger-like motif could take place to promote catalysis once the active DFF40 (CAD) dimer is assembled.

The very deep active site crevice seen in the crystal structure of activated DFF40 (CAD) requires that the linker DNA reaches the active site residues situated at the bottom of this crevice. This on the one hand provides a good explanation of how the enzyme might discriminate between poorly accessible DNA wrapped around histones and freely accessible internucleosomal DNA (28), but on the other hand the question arises how DNA approaches the bottom of the deep active site crevice at all. Activation of DNA-bound DFF stimulates the activity of released DFF40 (CAD) on naked DNA and on isolated nuclei. It could well be that the function of preformed DFF-DNA complexes is to facilitate access of the substrate DNA to the very deep active site cleft of activated DFF40 (CAD), which after DFF activation only requires the self assembly of the nuclease dimer around the DNA. This model would explain why incubation of DFF with DNA prior to or concomitant with its activation by caspase-3 has a stimulating effect on the catalytic activity of (DFF40) CAD.

We find that DFF can associate with chromatin in transfected HeLa cells *in vivo* suggesting that nuclear DFF might be activated in the apoptotic cell in a DNA bound state (Fig. 7). The stimulation and association of DFF40 (CAD) with histone H1 and HMGB1 and 2 *in vitro* has already been demonstrated and it can be concluded from these studies that DFF40 (CAD) might be directed to the linker DNA in chromatin by histone H1 where internucleosomal DNA fragmentation occurs (6, 20, 21). Our data now indicate that in addition to binding and stimulation of DFF40 (CAD) by chromatin proteins, DFF can also directly interact with the DNA and this interaction stimulates the activity of DFF40 (CAD). Stimulation could be due to assembly of active dimeric DFF40 (CAD) around the DNA facilitating substrate access to the catalytic center (Fig. 7). This could mean that activation of DFF bound to the linker region of chromosomal DNA in the cell takes advantage of the close proximity of the nuclease subunit to the chromatin substrate, thus accelerating the execution of apoptotic DNA fragmentation. The DNA binding data presented here highlight a unique feature of DFF as a nuclease/inhibitor complex and suggest a very effective mode of DFF activation *in situ* during apoptosis.

Acknowledgments—We thank U. Konradi for expert technical assistance, M. Knoblauch and I. Schneider-Hüther for help in confocal laser scanning micrsocopy, G. Lüder for help in transmission electron microscopy, R. Zhang for providing the CTCF-GFP fusion construct, W. C. Earnshaw for the gift of pRSET-B-ICAD-L, X. Wang for the gift of caspase-3 cDNA, and G. H. Silva for critically reading the manuscript.

REFERENCES

1. Nagata, S. (2000) *Exp. Cell Res.* **256,** 12–18
2. Nagata, S., Nagase, H., Kawane, K., Mukae, N., and Fukuyama, H. (2003) *Cell Death Differ.* **10,** 108–116
3. Counis, M. F., and Torriglia, A. (2000) *Biochem. Cell Biol.* **78,** 405–414
4. Wyllie, A. H. (1980) *Nature* **284,** 555–556
5. Liu, X., Zou, H., Slaughter, C., and Wang, X. (1997) *Cell* **89,** 175–184
6. Liu, X., Li, P., Widlak, P., Zou, H., Luo, X., Garrard, W. T., and Wang, X. (1998) *Proc. Natl. Acad. Sci. U. S. A.* **95,** 8461–8466
7. Enari, M., Sakahira, H., Yokoyama, H., Okawa, K., Iwamatsu, A., and Nagata, S. (1998) *Nature* **391,** 43–50
8. Sakahira, H., Iwamatsu, A., and Nagata, S. (2000) *J. Biol. Chem.* **275,** 8091–8096
9. Sakahira, H., and Nagata, S. (2002) *J. Biol. Chem.* **277,** 3364–3370
10. Sakahira, H., Enari, M., and Nagata, S. (1998) *Nature* **391,** 96–99
11. Thomas, D. A., Du, C., Xu, M., Wang, X., and Ley, T. J. (2000) *Immunity* **12,** 621–632
12. Sharif-Askari, E., Alam, A., Rheaume, E., Beresford, P. J., Scotto, C., Sharma, K., Lee, D., DeWolf, W. E., Nuttall, M. E., Lieberman, J., and Sekaly, R. P. (2001) *EMBO J.* **20,** 3101–3113
13. Widlak, P. (2000) *Acta Biochim. Pol.* **47,** 1037–1044
14. Lechardeur, D., Drzymala, L., Sharma, M., Zylka, D., Kinach, R., Pacia, J., Hicks, C., Usmani, N., Rommens, J. M., and Lukacs, G. L. (2000) *J. Cell Biol.* **150,** 321–334
15. Samejima, K., and Earnshaw, W. C. (1998) *Exp. Cell Res.* **243,** 453–459
16. Ramuz, O., Isnardon, D., Devilard, E., Charafe-Jauffret, E., Hassoun, J., Birg, F., and Xerri, L. (2003) *Int. J. Exp. Pathol.* **84,** 75–81
17. Samejima, K., and Earnshaw, W. C. (2000) *Exp. Cell Res.* **255,** 314–320
18. Durrieu, F., Samejima, K., Fortune, J. M., Kandels-Lewis, S., Osheroff, N., and Earnshaw, W. C. (2000) *Curr. Biol.* **10,** 923–926
19. Widlak, P., Li, P., Wang, X., and Garrard, W. T. (2000) *J. Biol. Chem.* **275,** 8226–8232
20. Liu, X., Zou, H., Widlak, P., Garrard, W., and Wang, X. (1999) *J. Biol. Chem.* **274,** 13836–13840
21. Toh, S. Y., Wang, X., and Li, P. (1998) *Biochem. Biophys. Res. Commun.* **250,** 598–601
22. Scholz, S. R., Korn, C., Gimadutdinow, O., Knoblauch, M., Pingoud, A., and Meiss, G. (2002) *Nucleic Acids Res.* **30,** 3045–3051
23. Meiss, G., Scholz, S. R., Korn, C., Gimadutdinow, O., and Pingoud, A. (2001) *Nucleic Acids Res.* **29,** 3901–3909
24. Samejima, K., Tone, S., Kottke, T. J., Enari, M., Sakahira, H., Cooke, C. A., Durrieu, F., Martins, L. M., Nagata, S., Kaufmann, S. H., and Earnshaw, W. C. (1998) *J. Cell Biol.* **143,** 225–239
25. Mattern, K. A., van der Kraan, I., Schul, W., de Jong, L., and van Driel, R. (1999) *Exp. Cell Res.* **246,** 461–470
26. Korn, C., Scholz, S. R., Gimadutdinow, O., Pingoud, A., and Meiss, G. (2002) *Nucleic Acids Res.* **30,** 1325–1332
27. Sakahira, H., Takemura, Y., and Nagata, S. (2001) *Arch Biochem. Biophys.* **388,** 91–99
28. Woo, E. J., Kim, Y. G., Kim, M. S., Han, W. D., Shin, S., Robinson, H., Park, S. Y., and Oh, B. H. (2004) *Mol. Cell* **14,** 531–539
29. Widlak, P., Lanuszewska, J., Cary, R. B., and Garrard, W. T. (2003) *J. Biol. Chem.*
30. Dunn, K. L., Zhao, H., and Davie, J. R. (2003) *Exp. Cell Res.* **288,** 218–223
31. Drew, H. R., and Travers, A. A. (1984) *Cell* **37,** 491–502
32. Ruiz-Carrillo, A., and Renaud, J. (1987) *EMBO J.* **6,** 401–407
33. Cote, J., Renaud, J., and Ruiz-Carrillo, A. (1989) *J. Biol. Chem.* **264,** 3301–3310
34. Suck, D., and Oefner, C. (1986) *Nature* **321,** 620–625
35. Doherty, A. J., Worrall, A. F., and Connolly, B. A. (1995) *J. Mol. Biol.* **251,** 366–377
36. Hsia, K. C., Chak, K. F., Liang, P. H., Cheng, Y. S., Ku, W. Y., and Yuan, H. S. (2004) *Structure* (*Camb*) **12,** 205–214
37. Li, C. L., Hor, L. I., Chang, Z. F., Tsai, L. C., Yang, W. Z., and Yuan, H. S. (2003) *EMBO J.* **22,** 4014–4025
38. Garinot-Schneider, C., Pommer, A. J., Moore, G. R., Kleanthous, C., and

James, R. (1996) *J. Mol. Biol.* **260,** 731–742
39. Hartley, R. W. (2001) *Methods Enzymol.* **341,** 599–611
40. Buckle, A. M., Schreiber, G., and Fersht, A. R. (1994) *Biochemistry* **33,** 8878–8889
41. Raines, R. T. (1998) *Chem. Rev.* **98,** 1045–1066
42. Kobe, B., and Deisenhofer, J. (1996) *J. Mol. Biol.* **264,** 1028–1043
43. Haigis, M. C., Kurten, E. L., and Raines, R. T. (2003) *Nucleic Acids Res.* **31,** 1024–1032
44. Kleanthous, C., and Walker, D. (2001) *Trends Biochem. Sci.* **26,** 624–631
45. Kleanthous, C., Kuhlmann, U. C., Pommer, A. J., Ferguson, N., Radford, S. E., Moore, G. R., James, R., and Hemmings, A. M. (1999) *Nat. Struct. Biol.* **6,** 243–252
46. Ko, T. P., Liao, C. C., Ku, W. Y., Chak, K. F., and Yuan, H. S. (1999) *Structure Fold. Des.* **7,** 91–102
47. Gu, J., Dong, R. P., Zhang, C., McLaughlin, D. F., Wu, M. X., and Schlossman, S. F. (1999) *J. Biol. Chem.* **274,** 20759–20762
48. McCarty, J. S., Toh, S. Y., and Li, P. (1999) *Biochem. Biophys. Res. Commun.* **264,** 176–180
49. Cheng, Y. S., Hsia, K. C., Doudeva, L. G., Chak, K. F., and Yuan, H. S. (2002) *J. Mol. Biol.* **324,** 227–236

Enzyme Catalysis and Regulation:

Interaction of DNA Fragmentation Factor (DFF) with DNA Reveals an Unprecedented Mechanism for Nuclease Inhibition and Suggests That DFF Can Be Activated in a DNA-bound State

Christian Korn, Sebastian R. Scholz, Oleg Gimadutdinow, Rudi Lurz, Alfred Pingoud and Gregor Meiss

J. Biol. Chem. 2005, 280:6005-6015.
doi: 10.1074/jbc.M413035200 originally published online November 30, 2004
